



ELSEVIER

Available online at [www.sciencedirect.com](http://www.sciencedirect.com)

SCIENCE @ DIRECT®

PHYSICS LETTERS B

Physics Letters B 553 (2003) 197–203

[www.elsevier.com/locate/npe](http://www.elsevier.com/locate/npe)

## The wobbling mode in $^{167}\text{Lu}$

H. Amro<sup>a,b,c</sup>, W.C. Ma<sup>a</sup>, G.B. Hagemann<sup>b</sup>, R.M. Diamond<sup>d</sup>, J. Domscheit<sup>e</sup>, P. Fallon<sup>d</sup>,  
A. Görgen<sup>d</sup>, B. Herskind<sup>b</sup>, H. Hübel<sup>e</sup>, D.R. Jensen<sup>b</sup>, Y. Li<sup>a</sup>, A.O. Macchiavelli<sup>d</sup>,  
D. Roux<sup>a</sup>, G. Sletten<sup>b</sup>, J. Thompson<sup>a</sup>, D. Ward<sup>d</sup>, I. Wiedenhöver<sup>f</sup>, J.N. Wilson<sup>b</sup>,  
J.A. Winger<sup>a</sup>

<sup>a</sup> *Mississippi State University, Mississippi State, MS 39762, USA*

<sup>b</sup> *The Niels Bohr Institute, Blegdamsvej 17, DK-2100 Copenhagen, Denmark*

<sup>c</sup> *Wright Nuclear Structure Laboratory, Yale University, New Haven, CT 06520-8124, USA*

<sup>d</sup> *Lawrence Berkeley National Laboratory, Berkeley, CA 94720, USA*

<sup>e</sup> *ISKP, University of Bonn, Nussallee 14-16, D-53115 Bonn, Germany*

<sup>f</sup> *Florida State University, Tallahassee, FL 32306-4350, USA*

Received 31 October 2002; received in revised form 10 December 2002; accepted 10 December 2002

Editor: J.P. Schiffer

### Abstract

High spin states in  $^{167}\text{Lu}$  were populated through the  $^{123}\text{Sb}(^{48}\text{Ca}, xn)$  reaction at 203 MeV. Four, presumably triaxial, strongly deformed (TSD) bands have been found in this nucleus. Several transitions linking an excited TSD band (TSD2) to the lowest (yrast) TSD band (TSD1) were observed. The electromagnetic properties of the connecting transitions have been investigated. Evidence for the assignment of TSD2 as a wobbling mode built on TSD1 is presented. This assignment is based on comparisons of the experimental data to theoretical calculations. The wobbling mode of excitation is an unambiguous signal of a stable triaxial deformation associated with these bands.

© 2002 Elsevier Science B.V. Open access under [CC BY license](#).

PACS: 27.70.+q; 21.10.Re; 23.20.En

Keywords: Triaxial deformation; Wobbling mode

The symmetry breaking associated with stable triaxial nuclei opens a new dimension to study collective nuclear rotation in which the rotation of the axially symmetric nuclei becomes a limit to a general description. Triaxial deformed nuclei with moments of inertia  $J_x > J_y, J_z$  can rotate about any of the prin-

cipal axes, although it is energetically favoured to rotate about the axis with the largest moment of inertia. A low-lying collective excitation associated with this symmetry reduction which is uniquely related to the rotational motion of a triaxial deformed nucleus is expected [1]. This is called the wobbling mode, described as a deviation of the axis of collective rotation away from the principal axis with largest moment of inertia. In the high spin limit, this precessional mo-

*E-mail address:* [hanan.amro@yale.edu](mailto:hanan.amro@yale.edu) (H. Amro).

tion, which has the character of a harmonic vibration, introduces a sequence of wobbling bands with increasing number of wobbling quanta,  $n_w = 0, 1, 2, \dots$ . The energy of a wobbling phonon, in the absence of intrinsic angular momentum or alignment, can be written as  $\hbar\omega_w = \hbar\omega_{\text{rot}} J \sqrt{(J_x - J_y)(J_x - J_z)/(J_y J_z)}$  with  $\hbar\omega_{\text{rot}} = \hbar^2 I / J_x$  [1]. Wobbling bands are expected to have structures similar to that of the  $n_w = 0$  band. Furthermore, a characteristic decay pattern between wobbling bands via  $\Delta I = \pm 1$  transitions, with large values of  $B(E2)_{\text{out}}$ , in competition with the in-band  $\Delta I = 2$  transitions is expected.

Cranking calculations with the ‘Ultimate Cranker’ code (UC) [2,3], based on a modified harmonic oscillator potential, predict local minima in the total energy surface with large quadrupole deformations,  $\epsilon_2 \sim 0.4$ , and pronounced triaxiality,  $\gamma \sim \pm 20^\circ$ , for nuclei with  $Z \sim 71$  and  $N \sim 94$ . These nuclei constitute a region of exotic shapes coexisting with normal prolate deformation [4,5]. The cranking calculations predict triaxial minima for all combinations of parity ( $\pi$ ) and signature ( $\alpha$ , where  $I = \alpha \bmod 2$ ). These calculations describe rotations about one of the principal axes and therefore preserve the signature symmetry. The deviation of the axis of collective rotation away from the principal axis, as described above in the wobbling mode, breaks this symmetry in the intrinsic frame. The principal axis cranking, UC, calculations cannot describe the wobbling degree of freedom. These calculations, though, can provide estimate of the local minimum for a triaxial shape. In this minimum, it is possible to investigate the spectrum of quasiparticle excitations, i.e., excitation energy and relative alignment for the possible combinations of signature and parity. The lowest of these configurations, with  $(\pi, \alpha) = (+, +1/2)$ , corresponds to an aligned  $i_{13/2}$  proton. The wobbling degree of freedom could be realized in the particle-rotor model (PRM) calculations where the  $i_{13/2}$  proton is coupled to a triaxial rotor with a shape corresponding to the local minimum found in the UC calculations. Fig. 1 illustrates a calculated total energy surface in  $^{167}\text{Lu}$ . Experimentally, several rotational strongly deformed bands have been observed in this mass region and presumed as triaxial strongly deformed (TSD) bands. The triaxiality associated with these bands could only be inferred from comparisons of their measured properties such as their excitation energies and quadrupole mo-

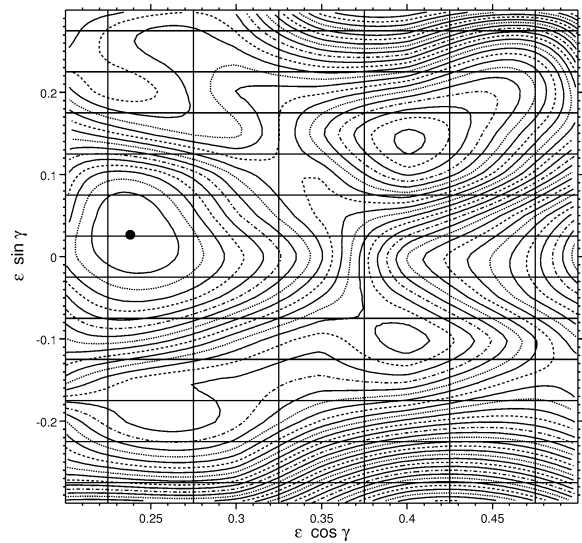


Fig. 1. Calculated potential energy surface for the  $(\pi, \alpha) = (+, +1/2)$  configuration in  $^{167}\text{Lu}$  at  $I = 97/2 \hbar$ . The energy difference between the contour lines is 0.2 MeV. The ND minimum at  $(\epsilon \sim 0.25, \gamma = 0^\circ)$  and the two local minima at  $(\epsilon_2 \sim 0.43, \gamma \sim \pm 20^\circ)$  are clearly seen.

ments with theoretical expectations. In the even- $N$   $^{163-167}\text{Lu}$  isotopes, these bands were interpreted as most likely corresponding to the  $\pi i_{13/2}$  intruder configuration [4–7]. The  $\pi i_{13/2}$  configuration is also involved in the TSD bands observed in  $^{164}\text{Lu}$  [8]. Three TSD bands were observed in  $^{168}\text{Hf}$  [9] and several TSD bands in the heavier Hf isotopes were recently reported [10,11]. To substantiate the large deformation associated with these bands, the transition quadrupole moments have been measured for the yrast TSD bands in several Lu isotopes [4,12,13] and in  $^{168}\text{Hf}$  [9]. The measured quadrupole moments are considerably larger than those of the normal deformed (ND) bands in this mass region. Only recently, firm evidence for the wobbling mode, and thereby triaxiality, was established in  $^{163}\text{Lu}$  for a one- and two-phonon wobbling excitations [14,15]. New evidence for the wobbling mode is also reported in  $^{165}\text{Lu}$  [16].

In this Letter we report on the experimental evidence for the wobbling mode in  $^{167}\text{Lu}$ . The detailed properties of the decay transitions from TSD2 to TSD1 band in  $^{167}\text{Lu}$  are presented. The comparison between those properties and theoretical expectations from particle-rotor model (PRM) calculations [17] of the wobbling mode in the presence of an aligned parti-

cle provides evidence for this mode in  $^{167}\text{Lu}$  with the excitation of one wobbling phonon, and therefore for the triaxiality associated with these bands.

The nucleus  $^{167}\text{Lu}$  was populated to very high spins through the  $^{123}\text{Sb}(^{48}\text{Ca}, 4n)$  reaction at 203 MeV. The  $^{48}\text{Ca}$  beam was provided by the 88-Inch cyclotron at Lawrence Berkeley National Laboratory. Gamma-ray coincidences were measured with the *Gammasphere* array which, at the time of the experiment, consisted of 100 Compton-suppressed Ge detectors. A total of  $2.2 \times 10^9$  events, requiring five or more suppressed Ge detectors in prompt coincidence, was collected and used in the off-line analysis. The coincidence events were sorted into a three-dimensional histogram (cube) using the Radware software package [18]. As a result of an extensive search through the coincidence cube, four presumably triaxial (TSD) bands have been found in  $^{167}\text{Lu}$ . Two of the new TSD bands are labelled as TSD1 and TSD2 in anticipation of the discussion to follow. A part of TSD1 confirms qualitatively the band

suggested in Ref. [7]. New results on the ND structure in  $^{167}\text{Lu}$  established from the current data set will be presented in a forthcoming publication [19].

The observed coincidences between transitions in TSD1 and TSD2 and transitions between the known ND states in  $^{167}\text{Lu}$  firmly establish that these bands belong to this nucleus. The population of these bands, relative to yrast, is  $\sim 8\%$  and  $\sim 2\%$ , respectively. Spectra of TSD1 and TSD2 are presented in Fig. 2. The large deformation associated with these bands is only inferred from their large  $J^{(2)}$  values as compared to those of the ND structure in  $^{167}\text{Lu}$ , in particular at lower frequency, as illustrated in the lower panel of Fig. 3, and the similarity to TSD bands in  $^{163}\text{Lu}$ . The observed fluctuation in the moment of inertia for TSD1 is due to band interactions with ND levels at both high and low spins and will be discussed in a later publication [20]. TSD1 was firmly linked to the ND structures in this nucleus via several transitions as illustrated in Fig. 4. More interestingly, TSD2

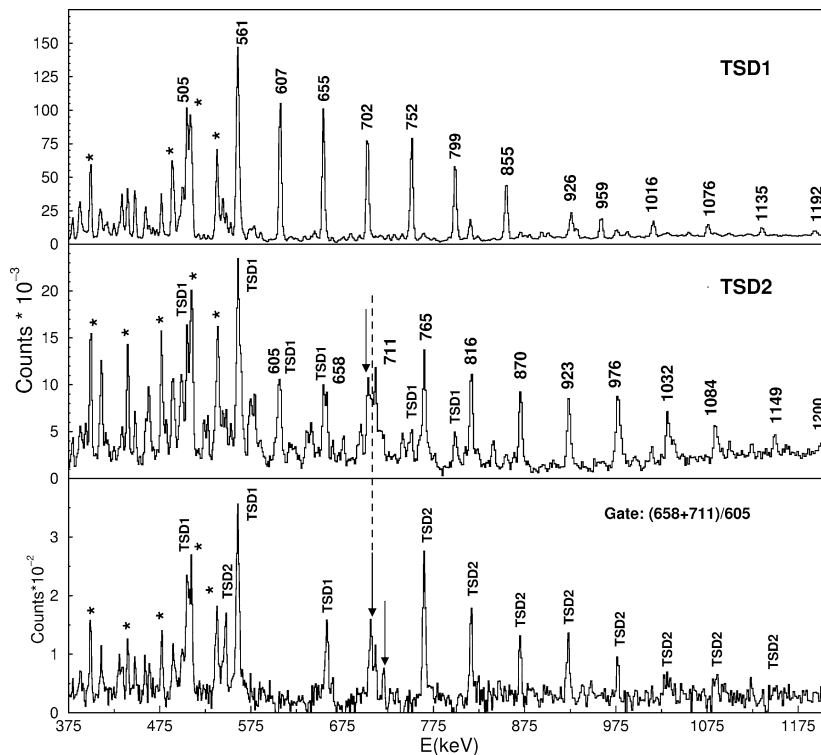


Fig. 2. Coincidence spectra obtained by double gating on all combinations of transitions in TSD1 (top) and TSD2 (middle) in  $^{167}\text{Lu}$ . The arrow in the middle spectrum marks the centroid of the 704, 706, and 708 keV inter-band transitions. The arrows in bottom spectrum, with narrow gates in TSD2 as indicated, mark the 708 and 720 keV inter-band transitions. The \* marks the known ND transitions in  $^{167}\text{Lu}$ .

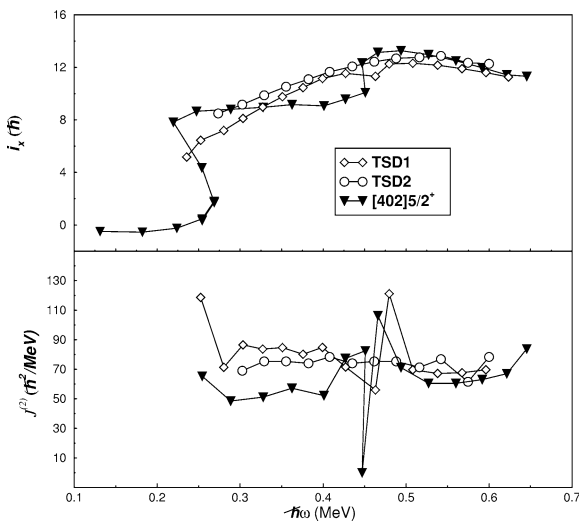


Fig. 3. Alignment  $i_x = I - I_{\text{ref}}$ , where  $I_{\text{ref}} = 35\hbar^2 \text{ MeV}^{-1} \omega + 45\hbar^4 \text{ MeV}^{-3} \omega^3$  (top), and the dynamic moment of inertia (bottom) as a function of rotational frequency for TSD1, TSD2, and the ND [402]5/2<sup>+</sup> bands in <sup>167</sup>Lu.

Table 1

Experimental values of branching ratio  $\lambda$ , mixing ratio  $\delta$ , and  $B(E2)_{\text{out}}/B(E2)_{\text{in}}$  for the inter-band transitions

$E_\gamma$ (keV)	$\lambda = \frac{I_\gamma(\Delta I=1)}{I_\gamma(\Delta I=2)}$	$\delta$	$\frac{B(E2)_{\text{out}}}{B(E2)_{\text{in}}}$
706.1	$0.91 \pm 0.04$	$-3.1^{+1.1}_{-3.4}$	$0.23^{+0.02}_{-0.05}$
704.2	$0.41 \pm 0.06$		
707.7	$0.39 \pm 0.04$	$(-5.1^{+1.6}_{-2.5})^a$	$0.26^{+0.03}_{-0.04}$
716.9	$0.30 \pm 0.08$		
730.3	$0.32 \pm 0.07$		

<sup>a</sup> Average from SpeeDCO analysis and angular distribution ratio.

decays to TSD1 instead of decaying to ND levels. Six transitions linking TSD2 with TSD1 were observed over a broad region of spin, see Fig. 4. Moreover, these transitions compete well with the in-band transitions of TSD2, see Table 1. The observed characteristic decay pattern of TSD2 via these linking transitions is quite similar to recent results in <sup>163,165</sup>Lu [14,16] and to theoretical expectations [17] of the decay out of a one-phonon to a zero-phonon wobbling band. Therefore, measuring the  $B(E2)_{\text{out}}/B(E2)_{\text{in}}$  values, by investigating the electromagnetic properties of the cross-band transitions, is crucial to establish TSD2 as a one-phonon wobbling band in <sup>167</sup>Lu.

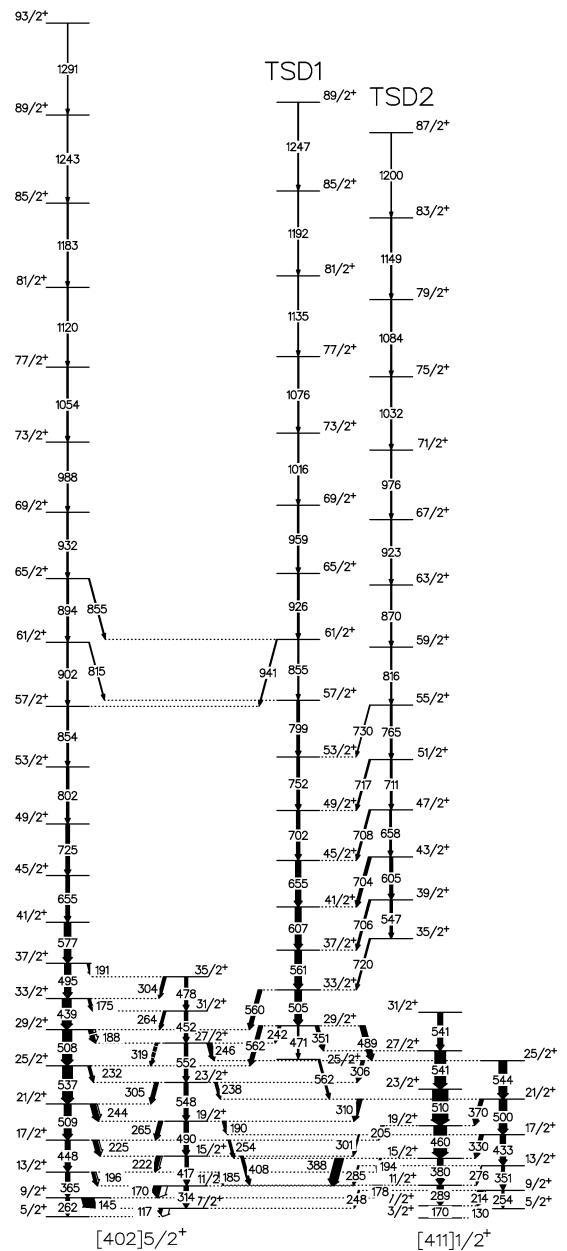


Fig. 4. Partial level scheme of <sup>167</sup>Lu. The ND bands are labelled with Nilsson quantum numbers.

To establish the spins and parities for TSD1 and TSD2, and multipolarity mixing ratios,  $\delta(E2/M1)$ , for the inter-band transitions, the full  $\gamma\gamma$  directional correlations from oriented states (DCO) [21] analysis was performed on the current data set. The analy-

sis is based on a transformation of the directional information into expansion coefficients of an orthogonal basis, and is referred to as the spectral expansion of DCO (SpeedCO) [22]. The data were sorted into 12 two-dimensional single-gated histograms of the expansion coefficients. For example, for the analysis of cross-band transitions from TSD2 to TSD1, clean gates on transitions in TSD2 and/or TSD1 were used in creating correlation matrices, and, subsequently clean gates in TSD2 and/or TSD1 were used to create double-gated correlation spectra. An angular distribution analysis was also performed, and the spin alignment for several stretched electric quadrupole (E2) transitions in both TSD and ND bands over a broad region of spin including that of the connecting transitions was established.

The stretched quadrupole character of the in-band transitions in TSD1 was firmly established. Based on that result and the fact that several links connect TSD1 to different ND levels at low spin, together with the mutual cross-band transitions observed around  $I = 61/2 \hbar$ , TSD1 has a firm parity and signature assignment  $(\pi, \alpha) = (+, +1/2)$ . The stretched quadrupole character of the in-band transitions in TSD2 was also confirmed. The  $\Delta I = 1$  mixed multipolarity character for three of the cross-band transitions was established. The alternative mixed multipolarity,  $\Delta I = 0$ , solutions could be rejected. Two solutions for the multipolarity mixing ratios,  $\delta(E2/M1)$ , for those transitions with either small or large negative values were measured. A polarization measurement from the current data set was not possible for these transitions. With both solutions measured for these mixing ratios, the alternative possibility with M2/E1 mixing in the linking transitions would result in unexpectedly large matrix elements for the M2 and, for the smaller solutions of  $\delta$ , also for the E1 transitions and is therefore ruled out. Based on these findings, parity and signature of  $(\pi, \alpha) = (+, -1/2)$  were assigned to TSD2, see Fig. 4. Our preference for the numerically larger solutions of  $\delta(E2/M1)$ , given in Table 1, is based on the almost identical behaviour of TSD2 and its decay to TSD1 in this nucleus and the one-phonon wobbling band in  $^{163}\text{Lu}$ , where the electric nature of the inter-band transitions was established from polarization measurements [14]. Therefore, the numerically smaller solutions of  $\delta(E2/M1)$ ,  $-0.26 \pm 0.16$ ,  $-0.07 \pm 0.07$ , and  $-0.35 \pm 0.65$  are

unlikely. The mixing ratios measured for the inter-band transitions are presented in Table 1. They correspond to rather large E2 components of 92–98% and small M1 contributions of 2–8%. The measured branching ratios and mixing ratios were used to extract the  $B(E2)_{\text{out}}/B(E2)_{\text{in}}$  values for the  $(E2; I \rightarrow I - 1)$  cross-band transitions. These quantities are also listed in Table 1.

With the spin, parity, and excitation energy established for TSD1 and TSD2, the overall similarity in alignment and dynamic moment of inertia as a function of frequency for these bands is demonstrated in Fig. 3, strongly suggesting that they have very similar structure, like their homologue TSD bands in  $^{163,165}\text{Lu}$  [14,16]. Fig. 5 illustrates the excitation energy of TSD1, TSD2, and the  $[402]5/2^+$  bands as a function of spin. It should be mentioned that it was not possible from coincidences considerations to firmly distinguish the top of TSD1 from that of the  $[402]5/2^+$  band above the  $61/2 \hbar$  level. According to Fig. 5, the excitation energy of TSD2 relative to TSD1 is only  $\sim 430$  keV at the lowest spins and decreases as spin increases. For the alternative choice of the top of TSD1, the excitation energy of TSD2 relative to TSD1 remains almost constant over the entire spin region where both bands were observed. The UC calculations predict the lowest configuration in the TSD well with  $(\pi, \alpha) = (+, +1/2)$  to correspond to the  $\pi i_{13/2}$  intruder orbital. This prediction is consistent with the measured parity and signature of TSD1. For the expected  $\pi i_{13/2}$  signature partner, cranking calculations with the UC code [2,3] predict a signature splitting of

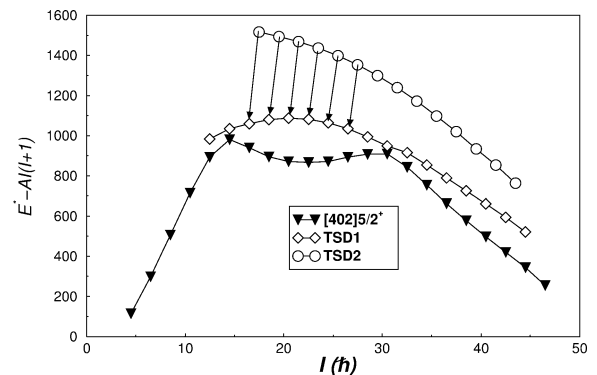


Fig. 5. Excitation energy minus a rigid-rotor reference for TSD1, TSD2, and the  $[402]5/2^+$  ND bands in  $^{167}\text{Lu}$ . The arrows represent the  $\Delta I = 1$  inter-band transitions.

$\sim 0.8$  MeV at the lowest spins, decreasing as spin increases due to gradual changes in the configuration. The local minimum associated with both signatures in the proton system is, within the spin range of interest, found at a similar quadrupole deformation and triaxiality ( $\epsilon_2 \sim 0.43$ ,  $\gamma \sim +19^\circ$ ). This would suggest that TSD1 and its signature partner have similar dynamic moments of inertia, as observed for TSD1 and TSD2, but the predicted excitation energy of a signature partner band is inconsistent with the observed excitation energy of TSD2 relative to TSD1 (only  $\sim 0.37$ – $0.47$  MeV). In addition, the alignment of the unfavored signature partner of TSD1 is expected to be  $\sim 1 \hbar$  lower than that of TSD1 which is inconsistent with the observed alignment of TSD2 relative to TSD1, see Fig. 3. Furthermore, the cranking-like solutions from the PRM calculations [17] for  $B(E2; I \rightarrow I - 1)$  and  $B(M1; I \rightarrow I - 1)$  [14] between signature partners have almost vanishing values, inconsistent with the measured  $B(E2)_{\text{out}}/B(E2)_{\text{in}}$  ratios which are, even with the smaller, unlikely solutions, for  $\delta$ , more than an order of magnitude larger. Based on these arguments, an interpretation of TSD2 as the unfavored signature partner of TSD1 is highly unlikely. An interpretation, from UC calculations, of TSD2 as a band built on a three-quasiparticle structure in which the  $i_{13/2}$  proton is coupled to a pair of neutrons with  $\alpha = 1$  with a minimum identical to that of TSD1 is also possible. Once again, the predicted excitation energy for such a band is similar to that of the signature partner and is inconsistent with the observed excitation energy for TSD2. Furthermore, the alignment gain for TSD2, as compared to that of TSD1, expected for such a three-quasiparticle structure, is inconsistent with the observed relative alignments of TSD2 and TSD1, see the upper panel of Fig. 3.

The most compelling interpretation of TSD2 is suggested by PRM. These calculations describe wobbling phonon excitations with  $n_w = 0, 1, 2, \dots$ , built on the aligned  $i_{13/2}$  proton configuration with  $n_w = 0$ . This excitation competes with the cranking-like signature partner. Moreover, according to these calculations, the following features are expected of the  $n_w = 1$  wobbling band: (a) moments of inertia and alignments very similar to those of the  $n_w = 0$  band; (b) decay to the  $n_w = 0$  band via  $\Delta I = \pm 1$  transitions with large  $B(E2; I \rightarrow I - 1)$  values which may dominate over M1 components; (c) these  $B(E2)$  values exhibit a de-

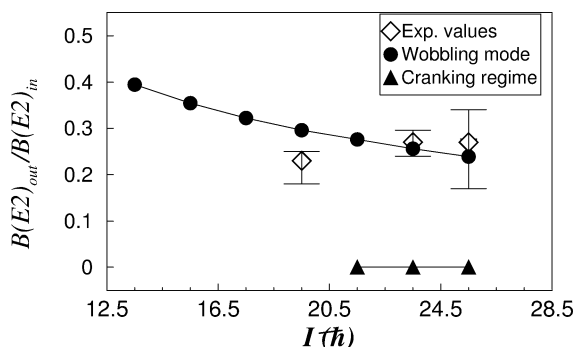


Fig. 6. Experimental  $B(E2)_{\text{out}}/B(E2)_{\text{in}}$  values for the  $I \rightarrow I - 1$  transitions from TSD2 to TSD1 in  $^{167}\text{Lu}$  together with the values calculated by the particle-rotor model [17].

pendence, in the high spin regime, on  $1/I$ , in contrast to their dependence on  $1/I^2$  in the cranking mode. The theoretical expectations, (a) and (b), agree quite well with the observed properties of TSD1, TSD2, and the linking transitions as illustrated in Figs. 3 and 5, and Table 1. Most importantly, the PRM estimates of the  $B(E2)_{\text{out}}/B(E2)_{\text{in}}$  values for the wobbling mode are found to be in good agreement with those measured in this work as can be clearly see in Fig. 6.

In conclusion, firm excitation energies, spin, and parity assignments were established for TSD1 and TSD2 bands in  $^{167}\text{Lu}$ . Moreover, TSD2 has been connected to TSD1 via several  $\Delta I = 1$  transitions. The measured electromagnetic properties of these linking transitions are in good agreement with the assignment of TSD2 as a one-phonon wobbling excitation built on TSD1. With the large  $B(E2)_{\text{out}}/B(E2)_{\text{in}}$  values measured for the decay out of TSD2, alternative interpretations as a signature partner or a band built on quasiparticle excitations could be ruled out. With the current results of a one-phonon wobbling excitation in  $^{167}\text{Lu}$ , four neutrons away from  $^{163}\text{Lu}$  where the one- and two-phonon wobbling excitations are already established [14,15], and new results of wobbling excitations in  $^{165}\text{Lu}$  [16], wobbling persists. Such persistence of the wobbling mode confirms triaxiality as a more general phenomenon in this region.

Although the wobbling mode is now firmly established in Lu nuclei, the exploration of the wobbling excitation mode and its interplay with microscopic degrees of freedom in a stable triaxial strongly deformed well is just at its beginning. It remains a challenge to experimentally establish the wobbling mode in an

even–even nucleus, which might shed more light on the role of particle alignment. It also remains a challenge to theorists to reproduce not only the  $B(E2; I \rightarrow I - 1)$  strength in the inter-band transitions for wobbling bands, but also the spin dependence of the excitation energies for those bands. Contrary to theoretical expectations, the observed excitation energies for the  $n = 1$  wobbling bands, relative to the yrast TSD band, decrease with increasing spin. Such a decrease may suggest a gradual change in the individual moments of inertia.

### Acknowledgements

Fruitful discussions with I. Hamamoto are gratefully acknowledged. The authors would like to thank the staff of the 88-Inch Cyclotron at LBNL. This research is supported by US DOE grants DE-FG02-95ER40939 (MSU), DE-FG02-91ER-40609 (Yale), and DE-AC03-76SF00098 (LBNL), the Danish Science Foundation, and the German BMBF under grant 06 BN 907.

### References

- [1] A. Bohr, B.R. Mottelson, Nuclear Structure, Vol. II, Benjamin, New York, 1975.
- [2] T. Bengtsson, Nucl. Phys. A 496 (1989) 56;  
T. Bengtsson, Nucl. Phys. A 512 (1990) 124.
- [3] R. Bengtsson, [www.matfys.lth.se/~ragnar/ultimate.html](http://www.matfys.lth.se/~ragnar/ultimate.html).
- [4] W. Schmitz, et al., Phys. Lett. B 303 (1993) 230.
- [5] H. Schnack-Petersen, Nucl. Phys. A 594 (1995) 175.
- [6] J. Domscheit, et al., Nucl. Phys. A 660 (1999) 381.
- [7] C.X. Yang, et al., Eur. Phys. J. A 1 (1998) 237.
- [8] S. Törmänen, et al., Phys. Lett. B 454 (1999) 8.
- [9] H. Amro, et al., Phys. Lett. B 506 (2001) 39.
- [10] D.J. Hartley, et al., in: Proceedings of the International Conference on Nuclear Structure, Wyoming, USA, 2002, p. 119.
- [11] A. Neußer, et al., Eur. Phys. J. A, in press.
- [12] G. Schönwaßer, et al., Eur. Phys. J. A 13 (2002) 291.
- [13] G. Schönwaßer, et al., Eur. Phys. J. A, in press.
- [14] S. Ødegård, et al., Phys. Rev. Lett. 86 (2001) 5866.
- [15] D.R. Jensen, et al., Phys. Rev. Lett. 89 (2002) 142503.
- [16] G. Schönwaßer, et al., in preparation.
- [17] I. Hamamoto, Phys. Rev. C 65 (2002) 044305.
- [18] D.C. Radford, Nucl. Instrum. Methods A 361 (1995) 297.
- [19] D. Roux, et al., in preparation.
- [20] H. Amro, et al., in preparation.
- [21] K.S. Krane, R.M. Steffen, R.M. Wheeler, Nucl. Data Tables 11 (1973) 351.
- [22] I. Wiedenhöver, et al., Phys. Rev. C 58 (1998) 721.